Boundary-Layer Meteorol (2017) 164:89–106
DOI 10.1007/s10546-017-0241-6

RESEARCH ARTICLE

Mechanisms Responsible for the Observed Thermodynamic Structure in a Convective Boundary Layer Over the Hudson Valley of New York State

Jeffrey M. Freedman[1] · **David R. Fitzjarrald**[1]

Received: 11 February 2016 / Accepted: 24 January 2017 / Published online: 11 February 2017

Abstract We examine cases of a regional elevated mixed layer (EML) observed during the Hudson Valley Ambient Meteorology Study (HVAMS) conducted in New York State, USA in 2003. Previously observed EMLs referred to topographic domains on scales of 10^5–10^6 km^2. Here, we present observational evidence of the mechanisms responsible for the development and maintenance of regional EMLs overlying a valley-based convective boundary layer (CBL) on much smaller spatial scales (<5000 km^2). Using observations from aircraft-based, balloon-based, and surface-based platforms deployed during the HVAMS, we show that cross-valley horizontal advection, along-valley channelling, and fog-induced cold-air pooling are responsible for the formation and maintenance of the EML and valley-CBL coupling over New York State's Hudson Valley. The upper layer stability of the overlying EML constrains growth of the valley CBL, and this has important implications for air dispersion, aviation interests, and fog forecasting.

Keywords Air-mass modification · Channelling · Convective boundary layer · Regional elevated mixed layer

1 Introduction

The structure and dynamics of the convective boundary layer (CBL) over flat, homogeneous terrain are well understood, but the presence of topography alters certain features (e.g. Choi et al. 2011; Ketterer et al. 2014). The daytime CBL in valleys exhibits considerable horizontal and vertical variability (Whiteman 1982; Schmidli 2013; Wagner et al. 2014; De Wekker and Koßmann 2015; Rendón et al. 2015) that influences mixing and transport of air masses above and below the CBL. How these differential advection effects sustain the simultaneous presence of different air masses in adjacent vertical layers has not been extensively docu-

✉ Jeffrey M. Freedman
jfreedman@albany.edu

[1] Atmospheric Sciences Research Center, University of Albany, State University of New York, Albany, NY 12203, USA

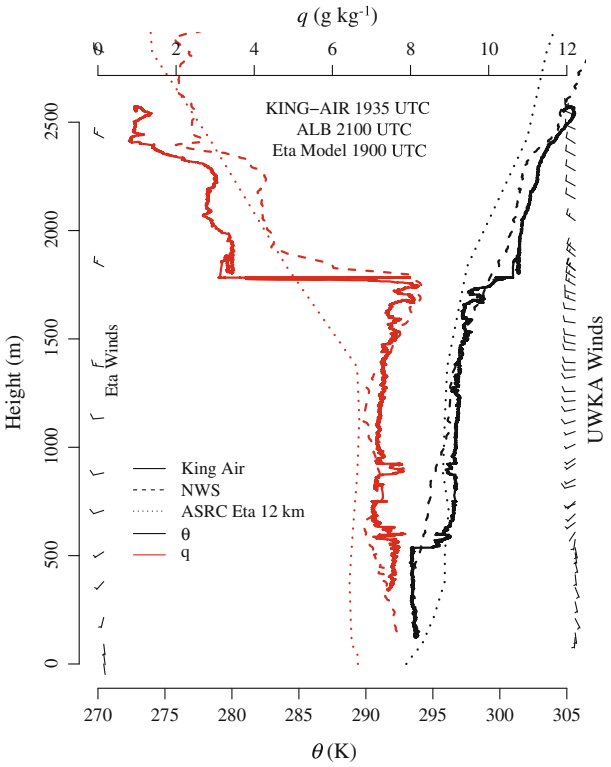

Fig. 1 Soundings of potential temperature (θ, in *red*) and specific humidity (q, in *black*) for 8 October 2003 from the National Weather Service Albany Forecast Office ("ALB", 2100 UTC, *dashed lines*), the King Air aircraft (1935 UTC, *solid lines*) and ASRC SKIRON/Eta Model (1900 UTC, *dotted lines*)

mented nor accurately depicted in mesoscale forecasting or air quality models (Hogrefe et al. 2001; Rao et al. 2003; Sofiev et al. 2011; Dai et al. 2014). In the Hudson Valley of New York State, this disjoint layering supports cross-valley horizontal advection of a regional elevated mixed layer (EML) overlying along-valley channelling. This leads to a baroclinic CBL that features directional wind shear and two distinct mixed layers: a regional EML overlying a valley-based CBL (e.g., Fig. 1).

Previous studies found evidence of multiple mixed layers—typically a well-mixed valley CBL with an inversion separating a weakly mixed, more stable layer above (e.g. De Wekker 2002; Emeis et al. 2008; Schmidli 2013). Emeis et al. (2008) observed that deep, relatively narrow Alpine valleys, where diurnally-driven up-valley and down-valley flows, interacting with the diurnal heating and cooling of steep terrain, generated multiple inversions. Schmidli (2013) showed that thermally-induced cross-valley circulations led to the development of a three-layer thermal structure as first noted by Whiteman (1982), a result of an interaction between top-down heating resulting from compensating subsidence in the stable valley core and bottom-up heating due to turbulent convection (Serafin and Zardi 2011). EMLs have also been observed in the western USA (Colorado Plateau; Arritt et al. 1992) and in Switzerland (Steinbacher et al. 2004). These examples, however, involve geographically large regions ($>3 \times 10^5\,\mathrm{km}^2$ for the Colorado Plateau; Arritt et al. 1992), or steep, mountainous terrain, such as the Swiss Alps (terrain >4000 m; Steinbacher et al. 2004), located adjacent to flat

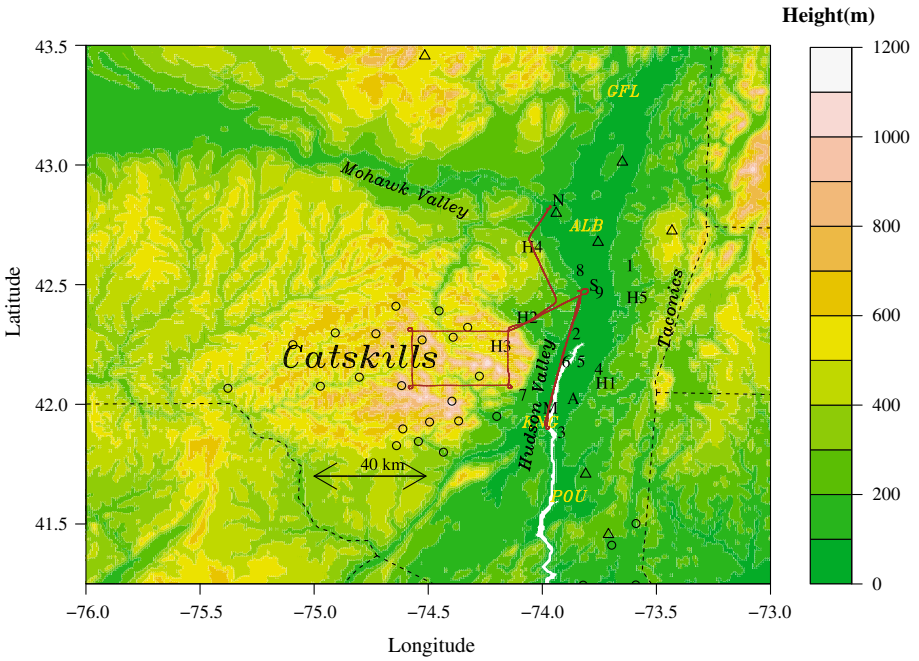

Fig. 2 Topographic map showing the HVAMS observation network with King Air afternoon CBL flight tracks. Surface stations include the NCAR ISFS numbered "1–9", HOBO stations "H1–H5", University of Alabama Mobile Integrated Profiling System (MIPS,."M"), NOAA profiler at Schenectady ("N"), ASRC SoDAR ("S"), ASRC Anchor Station ("A"), the New York City DEP network (*black open circles*), and the New York State Department of Environmental Conservation network (*black open triangles*). The locations of the cities of Albany ("ALB"), Poughkeepsie ("POU"), Glens Falls ("GFL"), and Kingston ("KNG") are also shown

plains. Finally, there are EMLs that have been implicated in severe convection in the Great Plains (Carlson et al. 1983) and the north-eastern USA (Banacos and Ekster 2010).

The temporal and spatial scales and mechanisms regarding formation of these EMLs differ from those observed during the Hudson Valley Ambient Meteorology Study (HVAMS). The regional EMLs observed over the Hudson Valley are much smaller in scale, occur over a plateau of modest elevation (<1000 m) and are generated locally. To our knowledge, the HVAMS represents the first documented example of a regional EML in the eastern USA.

The HVAMS was designed to examine how local topography and land-use patterns affect boundary-layer dynamics under predominantly fair-weather conditions. One focus of the project was the identification of mechanisms responsible for the development and maintenance of an EML and valley-CBL coupling as illustrated in Fig. 1. The physical processes responsible for the regional EML and valley-CBL coupling have been posited (De Wekker and Koßmann 2015), but the HVAMS represents the first time a field campaign has targeted resources, including a sufficiently dense instrumentation network, the use of remote sensing platforms, and aircraft-based measurements, enabling the identification of the features and mechanisms associated with the thermodynamic development and maintenance of a regional EML coupled with a valley CBL.

2 The Hudson Valley and Environs

The Hudson Valley (the "Valley") of New York State extends northwards more than 300 km from New York City to Glens Falls, New York (GFL; Fig. 2). Valley sidewalls range from less than 100 m at New York City and other locations to over 1000 m at the Catskill Mountain Escarpment, but generally rise 200–300 m above the Valley plain. From Albany southward to Poughkeepsie, which encompasses the length of the HVAMS domain (Fig. 2), the Valley is generally about 20–30 km wide. The Hudson River is a tidal estuary (part of the Hudson Fjord; Adams 1996) extending to the Atlantic Ocean. A 2-m tidal amplitude in the river is typical, with the bottomland elevation from Albany southwards only 3–5 m above sea level (a.s.l.). Thus, thermally-direct valley circulations (up-valley/down-valley flows) are negligible.

To the west of the Valley are the Catskill Mountains, a geologically eroded plateau (Ruedemann 1932), with the highest part of the escarpment (Slide Mountain at 1277 m) 35 km west of Kingston, New York. The Catskill Plateau varies between 300 and 1000 m in elevation, with an average height ≈500 m a.s.l. The east side of the valley generally has less relief, with the Taconic Mountains, around 20 km to the east of the river, rising to 700 m along the borders with southern Vermont, Massachusetts, and Connecticut.

Channelled flow in the Hudson Valley has been recorded in the written record since Henry Hudson's 1609 voyage (noted in Robert Juet's journal, as recounted in Lunny et al. 1959), and was quantitatively demonstrated as early as the 1820s (Hough 1855) and is evident from the HVAMS surface observations (Fig. 3). These channelled flows resemble those observed in the Rhine Valley in Germany (e.g., Groß and Wippermann 1987), and southerly winds in the valley beneath westerlies aloft dominate during the late spring through early autumn (Samson et al. 1975; Fitzjarrald and Lala 1989; Medeiros and Fitzjarrald 2014, 2015 see Fig. 3).

3 Field Deployment and Intensive Field Campaign

As part of the HVAMS, an intensive field campaign was conducted during autumn 2003; longer term HVAMS observations continued through 2006. Details of the HVAMS intensive field campaign surface station deployment, and other longer-term observational sites are given in Medeiros and Fitzjarrald (2014, 2015), summarized in Fig. 2, and are available at http://seabreeze.asrc.cestm.albany.edu/projects/HVAMS.htm. Here, we give a brief summary of the HVAMS observation platforms that are directly associated with the presented study.

3.1 Aircraft Measurements

The University of Wyoming King Air aircraft provided high-resolution measurements of wind, temperature, and humidity within and above the regional EML and valley CBL along and adjacent to the Hudson Valley and over the Catskill Plateau. During the HVAMS, the King Air employed a differential pressure gust-probe system (Rosemount 858AJ/831CPX) to sample aircraft-relative winds and an inertial navigation system (Honeywell Laseref SM) to sample aircraft attitude and motions relative to the Earth. Fast response (25 Hz) measurements of air temperature (Rosemount 102) and dew point (Cambridge Model 137C3) were made continuously. Turbulent measurements of momentum flux (Friehe type, with University of Wyoming modifications) and moisture flux (LICOR 6262) were also measured aboard the King Air, along with upward and downward irradiance (Eppley precision spectral pyra-

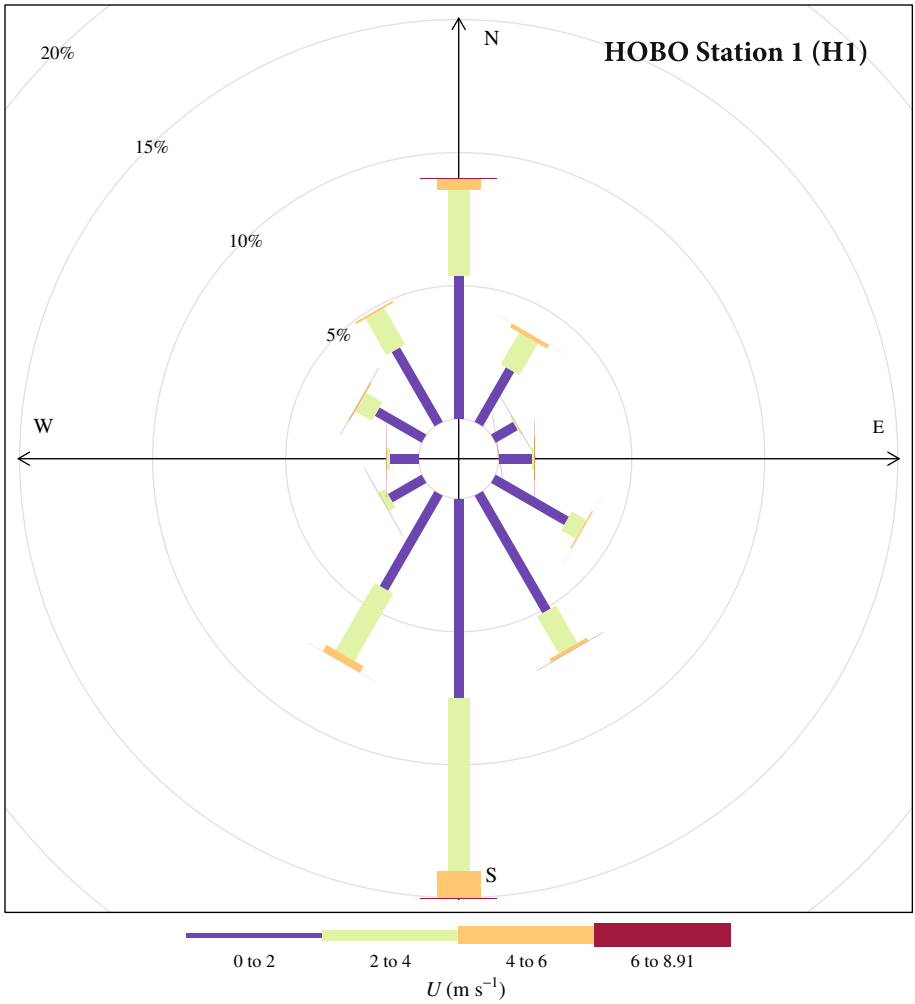

Fig. 3 Wind rose showing the frequency distribution of wind speed (U) and direction at HOBO station H1 for Days 150–270 (30 May–27 September) during years 2004 and 2005

nometer and precision infrared radiometer). Further details on the King Air system can be found at http://www.atmos.uwyo.edu/n2uw/.

Twenty-six flights of the King Air aircraft occurred on eighteen days during the period 1–31 October 2003. Specific flight plans were designed to capture the regional EML and valley-CBL coupling ("CBL structure flight"), with 18 separate afternoon profiles performed on 16 flight days. Along-valley and cross-valley legs of these flights provided high temporal and spatial resolution of vertical and horizontal measurements of scalars, and heat, moisture, and momentum fluxes, facilitating estimates of the horizontal advection of heat and moisture (see e.g. Mahrt et al. 2001; LeMone et al. 2002; Laubach and Fritsch 2002).

The afternoon CBL structure flights consisted of along-valley and cross-valley stacked legs and were flown between 1300 and 1700 local time (LT). (A few flights were combined with the CBL decay tracks that occurred later in the afternoon and into the evening.) Some flights

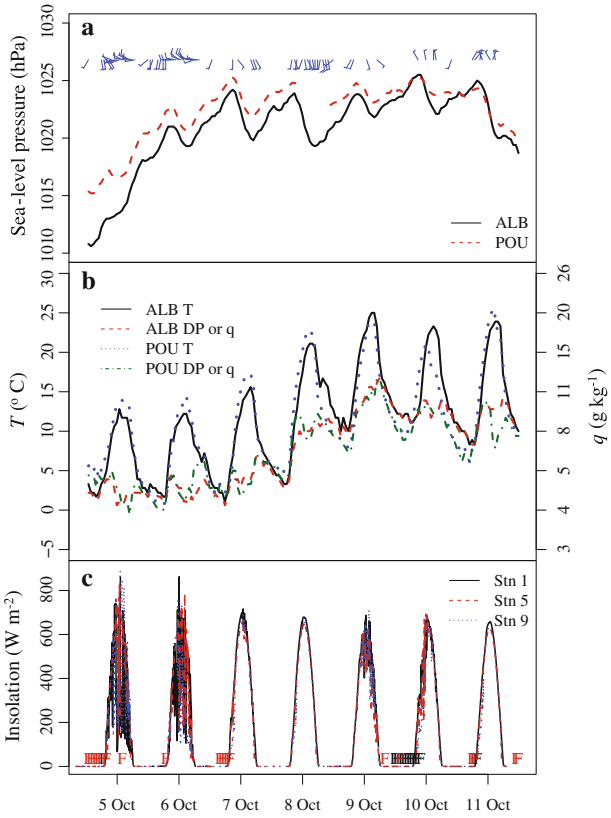

Fig. 4 **a** Albany ("ALB") and Poughkeepsie ("POU") ASOS daily sequence of hourly wind (1 barb = $5\,\mathrm{m\,s^{-1}}$), pressure (hPa), and precipitation (mm); **b** same as top, except for temperature (°C), dew point (°C) and specific humidity ($\mathrm{g\,kg^{-1}}$); **c** ISFS insolation ($\mathrm{W\,m^{-2}}$) and Albany and Poughkeepsie fog presence (indicated by symbols "F", *red* for Poughkeepsie, *black* for Albany)

included an additional box track over the Catskills (see Fig. 2). The along-valley flux legs were 80 km long, flown at altitudes of 0.2, 0.5, 0.8 and $1.2z_i$ (with z_i defined as the regional EML inversion base as determined from an initial King Air sounding). The cross-valley stacks (flown at the same levels) were used to estimate horizontal advection within and over the valley and to compare the thermodynamic characteristics of the EML and valley-CBL coupling at both the northern and southern ends of the HVAMS domain. Advection estimates were made using horizontal gradients from the along-valley and cross-valley flights. The box track (30 km × 30 km) was flown over the Catskills at a height $z \approx 0.8z_i$ to sample the thermodynamic characteristics of the plateau mixed layer.

3.2 National Center for Atmospheric Research (NCAR) Integrated Surface Flux System (ISFS)

During September to October 2003 a network of nine flux towers (see Fig. 4) from the NCAR ISFS group was deployed in the Valley (UCAR 2016). Real-time transmission of the 5-min statistics from each station via the Geostationary Operational Environmental Satellite (GOES-East) satellite provided about an 85–90% data recovery rate (except at station 5).

After the intensive field campaign, all ISFS stations were removed. Additional details are provided in Medeiros and Fitzjarrald (2014, 2015).

3.3 Automated Surface Observing System (ASOS) Stations

During the intensive field campaign, the surface station deployment was supplemented by measurements from surrounding ASOS stations, principally Poughkeepsie and Albany, operated by the National Oceanic and Atmospheric Administration (NOAA) National Weather Service (NWS) and Federal Aviation Administration. In addition to archiving regularly reported hourly ASOS reports, 1-min and 5-min observations for these stations were acquired from the Albany NWS Forecast Office and the NOAA National Climatic Data Center.

3.4 New York City Department of Environmental Protection (DEP) Surface Observation Network

The New York City DEP operates a network of more than 20 surface stations throughout New York City's upstate watersheds—most in the west-of-Hudson reservoir system (which contains 90% of the city's water supply capacity) on the Catskill Plateau. At the time of the HVAMS intensive field campaign, the DEP sites (see Fig. 2) provided measurements of temperature, humidity, wind speed and direction, irradiance, precipitation, snow depth, and soil moisture (Campbell Scientific 3-m tripod mounted stations). Most station elevations ranged between 300 and 600 m a.s.l., with one site, Winnisook Lake on Slide Mountain, located at an elevation of 1103 m a.s.l. One-hour averaged data from the DEP stations were used in this analysis.

3.5 Operational Soundings

To complement the Albany NWS Forecast Office operational 0000 UTC and 1200 UTC soundings, additional sondes were launched at 1400, 1700, and 2100 UTC on King Air flight days. The Albany NWS Forecast Office used Global Positioning System-type sondes providing high-resolution (5 m) profiles of temperature, humidity, and winds.

3.6 ASRC SKIRON/Eta Forecasts

The Atmospheric Sciences Research Center (ASRC) of the State University of New York at Albany developed a high-resolution (12 km) weather forecasting system based on the SKIRON/Eta numerical model for operational 48-hr weather forecasts over the eastern part of the USA (Cai et al. 2008). SKIRON/Eta model fields were used to drive the CAMx photochemical model for air quality forecasts. The CAMx-derived air quality forecasts were run with two nested grids at 36-km and 12-km horizontal resolution. Initialized model fields of temperature at levels approximating the midpoints of the regional EML and valley CBL were used to calculate the daily temperature advection presented in Sect. 5.3. The same initialization was used to for the vertical profile shown in Fig. 1.

4 Meteorological and Climatological Contexts

One goal of the HVAMS was to observe the evolution of air-mass modification sequences, where local exchange processes dominate CBL concentration tendencies (such as heat and moisture; Freedman and Fitzjarrald 2001; see Fig. 4). These sequences are a common occur-

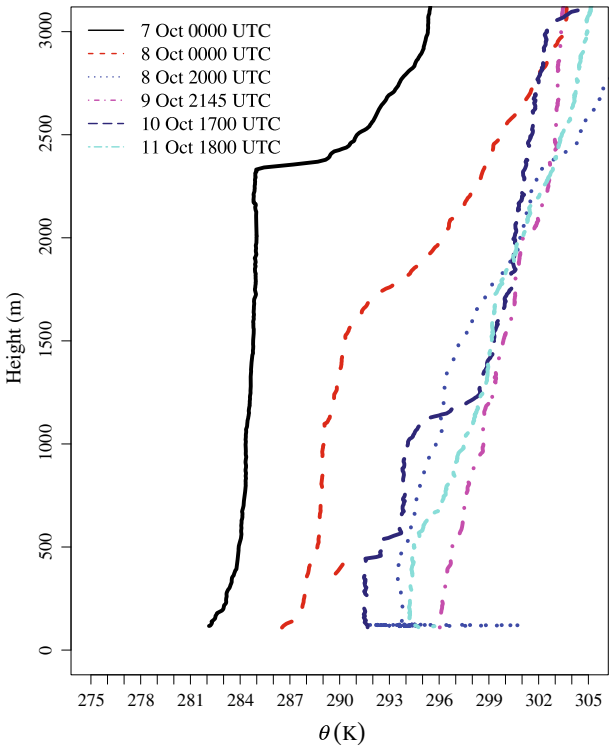

Fig. 5 NWS Albany afternoon (or evening) soundings of potential temperature (θ) for 7–11 October 2003

rence in the north-eastern USA, where a procession of frontal systems (usually one or two per week) moves across the region, ushering in drier and usually cooler air masses. The interval between frontal passages (about 3–5 days) allows the mixed layer to accumulate heat, moisture, and other trace gases over a period of several days. The presence of a residual layer following the day after a frontal passage facilitates rapid growth of the following morning's CBL and remixing of scalars from the previous day's diurnal cycle (Freedman and Fitzjarrald 2001), diminishing the role of entrainment of air from the free atmosphere above until the top of the residual layer is reached. However, the presence of the regional EML over the valley adds complexity to these boundary-layer processes during the sequence.

During the HVAMS intensive field campaign several such sequences occurred, including a six-day event spanning 6–11 October (Fig. 4). For this and the other sequences, regional EML and valley-CBL coupling becomes evident the day after a frontal passage (Fig. 5). At least nine days featured the occurrence of the regional EML and valley-CBL coupling (3, 6–11, 18, 25, and 31 October 2003). Here, we focus on the 6–11 October 2003 sequence.

Following a frontal passage on 5 October, an anticyclone over the western Great Lakes combined with an upper level trough located over Ontario, Canada and the north-eastern USA produced a north-westerly flow over the Hudson Valley region. A 2400-m deep CBL developed at Albany on the first full day following the frontal passage (Fig. 5). Subsequently, the surface anticyclone slowly moved eastwards, eventually intensifying over New England by 10 October, allowing for initially channelled northerly winds to change to southerly during 7–9 October, and then change back to northerly from 10 to 11 October (Fig. 4a). Flow aloft,

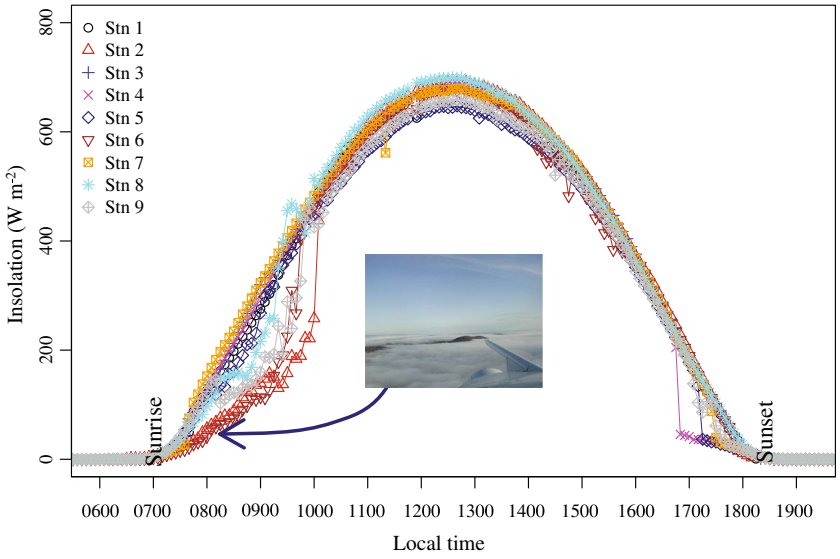

Fig. 6 ISFS 5-min surface insolation ($W\,m^{-2}$) for all stations on 8 October 2003; (*inset*): picture of Valley fog at 300 m above sea level (a.s.l.) near ISFS station 6 taken by King Air aircraft pilot Tom Drew at 0815 LT (1215 UTC). *Arrow* points to ISFS station 6 insolation observation at 0815 LT

except for transient periods, was perpendicular or oblique (westerly on 5–9 October; easterly on 10–11 October) to the axis of the valley throughout the sequence.

Near-calm conditions allowed for the development of morning fog during this sequence (Fig. 4c). The southern part of the HVAMS domain appeared to be a more favoured region for fog development (noted in satellite imagery and during the early morning King Air flights; see Fig. 6), perhaps because of the higher valley walls in this area, in contrast to the more open terrain in the northern part of the valley (Fig. 2).

5 Mechanisms

We propose three principal mechanisms operating separately or in tandem leading to the development of the regional EML and subsequent coupling to the valley CBL: (1) the presence of early morning fog that reduces the total available buoyant energy for boundary-layer growth; (2) advection of warmer air from the Catskill Plateau over the Valley; and (3) the channelling of flow within the Valley that serves to maintain low-level ambient conditions (temperature and humidity). Except for (2), these mechanisms differ from those observed or modelled in previous studies of primarily Alpine valleys referenced earlier, particularly with respect to the additional precursor conditions (cool-air pooling, fog and channelling) necessary for the development of the regional EML. The following discussion focuses on how the interplay of these processes initiates the formation and subsequent maintenance of the observed regional EML and valley-CBL coupling.

5.1 The Role of Fog

During autumn, fog is common in the Hudson Valley (Fitzjarrald and Lala 1989), reducing surface heat fluxes that, at least initially, warm the ground, dissipate the early morning surface inversion, and drive mixed-layer growth (e. g., Fig. 6, Fitzjarrald and Lala 1989). Surface

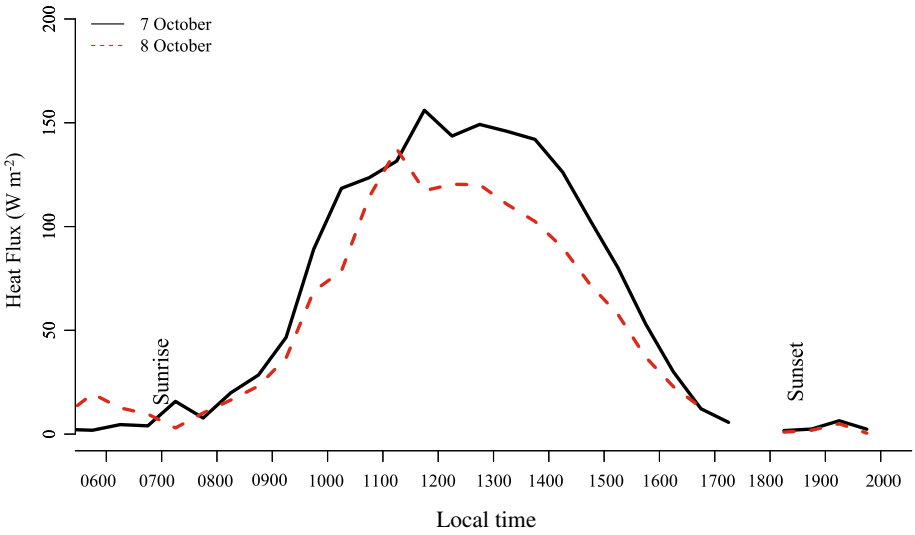

Fig. 7 ISFS network-averaged surface heat fluxes (W m^{-2}) for 7 (*solid black line*) and 8 (*dashed red line*) October 2003. Local sunrise and sunset times indicated by *text*

insolation measured at the ISFS stations (Fig. 6), surface visibility observations from Albany and Poughkeepsie ASOS stations (Fig. 4c), and visual observations (see e.g. Fig. 6 [inset]) from the early morning King Air flights indicate that, when present, fog persisted until about 1300 UTC (0900 LT). Maximum ISFS network-averaged sensible heat fluxes reached about 150 W m^{-2} (Fig. 7), inversion depths were about 200 m and the surface inversion strength ($\Delta\theta_v$, where θ_v is the virtual potential temperature) averaged about 7 K (Fig. 8a, b). Calculations using the integral method (Garratt 1992) indicate that the time to erode the inversion, given by

$$t = \left[(T h_i \Delta\theta_v) / \left(\overline{w'\theta_v'} \right)_n \right]^{1/2}, \tag{1}$$

is approximately 3.1 h, where $T \approx 3$ h, h_i is the height of the surface inversion, and $\left(\overline{w'\theta_v'} \right)_n$ is the network average (subscript "n") midday surface buoyancy flux (140 W m^{-2}; see Fig. 7). Sunrise during the intensive field campaign varied from 0650 LT to 0720 LT. On days without fog the surface inversion dissipated by mid-morning (approximately 1030 LT), in agreement with integral method estimates (see Fig. 8a). Supplementary analysis using the time at which the 2-m ISFS network-averaged θ exceeds that at 200 m as determined from the King Air and NWS soundings (see Angevine et al. 2001) showed similar results.

Soundings on fog days indicate that the surface inversion did not fully erode until noon or shortly thereafter (see Fig. 8b; Fitzjarrald and Lala 1989; Meyer and Lala 1990; Haeffelin et al. 2010), about 2 h after the fog had dissipated (evident from the observed surface insolation in Fig. 6). Thus, with morning fog, only about 2–4 h of positive buoyancy flux is available on the valley floor to drive CBL growth before a low sun angle results in decaying convective conditions by 1600 LT (Fig. 7).

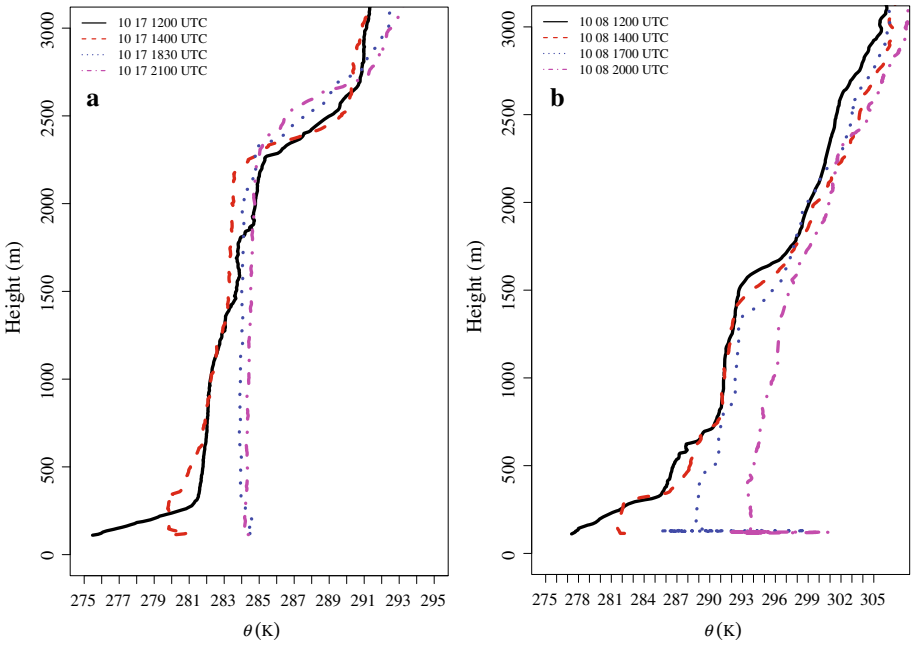

Fig. 8 **a** NWS Albany afternoon soundings of potential temperature (θ) for 17 October 2003; **b** same as **a** except for 8 October 2003

5.2 The Catskill Plateau Regional EML and Valley CBL

The elevated terrain of the Catskill Plateau experiences earlier leaf senescence and hence reduction in evapotranspiration than occurs in the adjacent lowlands of the Hudson Valley. This is confirmed by the similarity in seasonal evapotranspiration trends (Fitzjarrald et al. 2001) at Harvard Forest (Foster 1992), an elevated site (353 m) in central Massachusetts (Moore et al. 1996; Sakai et al. 1997). Both regions, at similar latitudes, elevation, and within 200 km of each other, experience similar weather and climate (Thayer 1996; Freedman 2000). Consequently, during October, sensible heat fluxes are greater at the Catskill Plateau than at the valley floor (Czikowsky and Fitzjarrald 2004), resulting in higher θ and lower specific humidity (q) than are found within the Valley (Czikowsky 2003). The Catskill Plateau is the expected source region for the regional EML.

The DEP stations, combined with King Air observations, are used as a surrogate "profile" of θ to determine if the Catskill Plateau-modified air mass is sufficiently warmer as compared with the valley CBL. Since there are no pressure measurements at the DEP stations, θ was determined using the hypsometric equation (Wallace and Hobbs 2006).

Following a frontal passage, the atmosphere encompassing both the Catskills and the Hudson Valley is well mixed by large-scale advective processes, resulting in little spatial variation in temperature or scalar concentrations. For example, on day 1 during the sequence shown in Fig. 9, θ at both the high elevation (1106 m a.s.l.) DEP site (station 148) and the lowest ISFS station (station 6, at 20 m a.s.l.) is virtually the same (Fig. 9a). Subsequently, local processes (e.g., accumulation of heat and moisture through air-mass modification) begin to dominate, and by day 3 the air over the Catskill Plateau is several K warmer and somewhat drier than corresponding heights over the Valley (Fig. 9a, b). With the prevailing synoptic

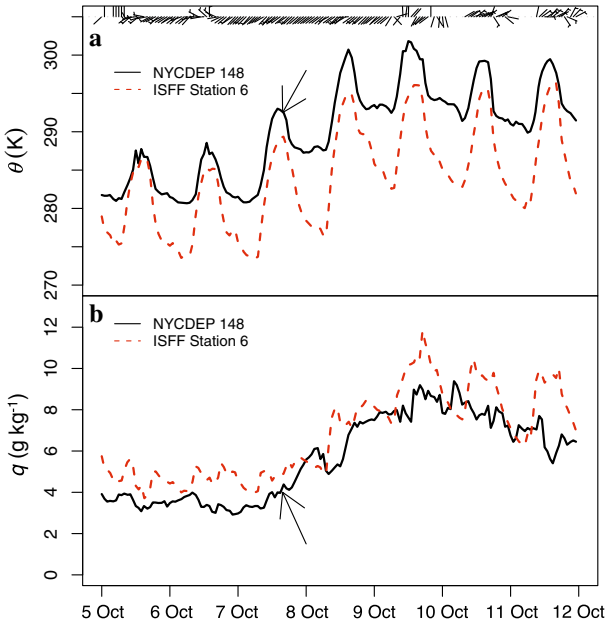

Fig. 9 **a** Sequence of hourly potential temperature (θ) and hourly wind (1 barb = 5 m s^{-1}) for DEP station 148 (*solid black line*) and ISFS station 6 (*dashed red line*) for 5–11 October 2003; **b** same as top except for specific humidity (g kg^{-1}). *Arrow* in (**a**) points to DEP station 148 θ value used in Fig. 10

flow, the locally generated CBL over the Catskill Plateau moves eastward over the Valley as a regional EML, while Valley flow is channelled along the north-south axis. The delayed onset of surface convective conditions in the Valley produces a shallow CBL, which is now topped by the warmer EML. Figure 10 shows how the warmer Catskill Plateau air produces an EML overlying the valley CBL. Here, we use hourly-averaged DEP surface station θ as observed at 2030 UTC (1630 LT), the peak afternoon temperature shown by the arrow in Fig. 9a. As the DEP temperature measurements are made at 2 m a.s.l., we assume that a superadiabatic surface layer results in a 1–2 K temperature excess compared with the average CBL θ. This produces a Catskill-generated CBL θ profile consistent with the NWS sounding in Fig. 10.

5.3 Horizontal Advection Estimates

To confirm and quantify the role that thermal advection plays in maintaining the observed regional EML and valley-CBL coupling, we estimated its contribution to each layer from the King Air and surface observations, and the SKIRON/Eta simulations, by

$$\frac{\partial \theta_{layer}}{\partial t} = -u_{layer}\frac{\partial \theta_{layer}}{\partial x} - v_{layer}\frac{\partial \theta_{layer}}{\partial y}, \tag{2}$$

where u and v represent the horizontal velocity components, and the subscript "layer" denotes that these are averages for each mixed layer (EML and valley CBL). It is assumed that radiative-flux divergence differences between the two layers are negligible.

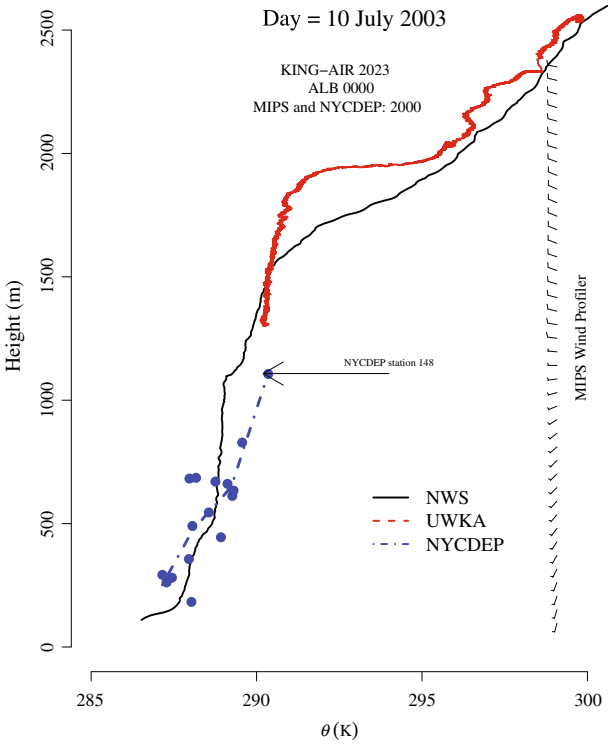

Fig. 10 Soundings of potential temperature (θ) from NWS Albany (0000 UT, *solid black line*) and the King Air (2023 UT, *solid red line*), 7 October 2003. Also plotted are DEP network stations θ estimates (see text for explanation) by altitude (*solid blue circles*). *Blue dot-dash* line shows smoothed profile

Table 1 Advection differential ($\times 10^{-5}$ K s^{-1}) as estimated from the King Air, ASRC SKIRON/Eta model, and differences between averaged temperatures at DEP stations above 500 m and the ISFS network

Date	King Air aircraft	Eta 12 km	ISFS–DEP surface stations
7 October	7.78	7.07	−0.35
9 October	1.7	5.32	6.36
10 October	−0.77	−3.96	3.82
20 October	8.32	18.9	1.73
25 October	6.28	7.31	12.17

5.3.1 King Air Estimates

The King Air aircraft estimates of thermal advection (Table 1) within the EML (as measured at $z = 0.8z_i$) indicate averaged values of 7.7×10^{-5} K s^{-1}, and -3.1×10^{-5} K s^{-1} in the valley CBL ($\approx z = 0.2z_i$). This differential (4 K day^{-1}) is sufficient to maintain and subsequently increase the strength of the elevated inversion ($\Delta\theta$ ranging between 2–6 K) over the valley.

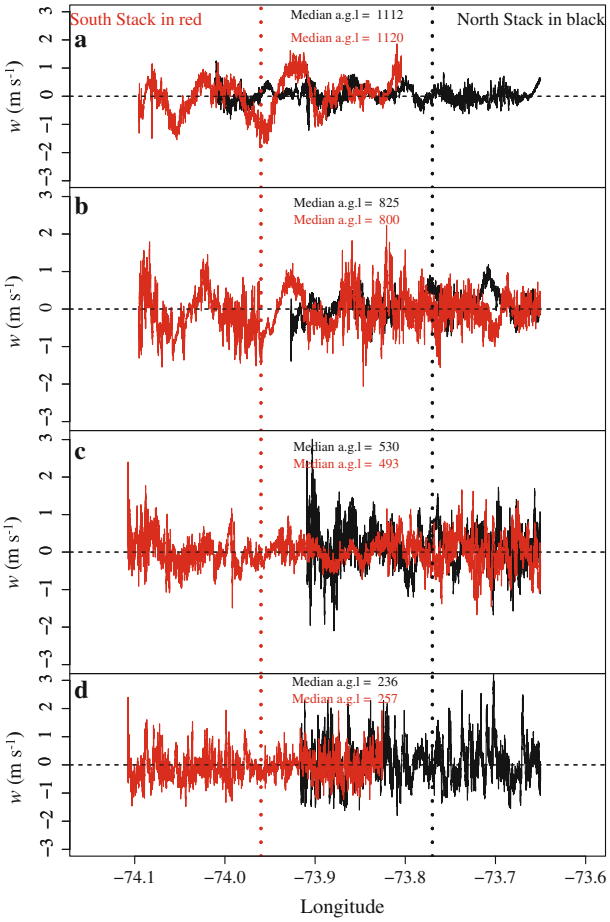

Fig. 11 Cross-valley vertical velocity (m s^{-1}) as measured by the King Air for upper regional EML (**a** and **b**) and lower valley CBL (**c** and **d**) for north stack (*black*) and south stack legs, 20 October 2003. Median altitudes a.g.l. for each leg are also shown

5.3.2 ISFS and DEP Surface Stations

Since warm air moving eastwards off the Catskill Plateau is one source for maintaining the strength of the elevated inversion over the Hudson Valley, differences between averaged temperatures at DEP stations above 500 m and the ISFS network were used to estimate the advection differential. These estimates provide a measurement constraint on the magnitude of the advection terms. Table 1 incorporates two days for which there are differences in the sign of the differential advection, 7 October and 10 October. (The negative values on 10 October are likely due to the easterly flow aloft—thus, there was no advection of Catskill Plateau air.) Otherwise, the estimates are comparable with the other methods used to calculate the Catskill Plateau-Valley temperature advection. Using the DEP and Valley surface station networks demonstrates a method for forecasting the probability of a regional EML and valley-CBL coupling developing, a technique that can be incorporated into operational numerical weather prediction forecasts.

Finally, time series for the 20 October 2003 King Air flight show distinct differences in turbulence intensity, represented by the instantaneous vertical velocity measurements between the mixed layers (Fig. 11). For this CBL flight, the King Air flew four stacked cross-valley legs in the north, depicted by the solid black lines at 1112 m (Fig. 11a), 825 m (Fig. 11b), 530 m (Fig. 11c), and 236 m (Fig. 11d), and four in the south, depicted by solid blue lines at 1120 m (Fig. 11a), 800 m (Fig. 11b), 493 m (Fig. 11c), and 257 m (Fig. 11d) to measure turbulence intensity just above and within the EML (Fig. 11a, b) and within the valley CBL (Fig. 11c, d). As the flow moves from the Catskill Plateau over the valley, turbulence decays from west-to-east (Fig. 11a, b), suggesting that the EML remains separate and distinct from the valley CBL (Fig. 11c, d), which exhibits little cross-valley difference in turbulence intensity (compare Fig. 11a, b with Fig. 11c, d). Valley processes discussed above (i.e. fog, radiational cooling and channelling) serve to maintain the two distinct mixed layers.

6 Conclusions

Three principal mechanisms operating in tandem are responsible for the regional elevated mixed layer (EML) and valley CBL coupling observed during the HVAMS (see Fig. 12): (1) channelled flow within the Valley; (2) advection of warmer and drier air from the Catskill Plateau; and (3) fog formation and/or nocturnal pooling of cooler air within the Valley. The development and maintenance of the regional EML and valley convective boundary layer (CBL) coupling occurs as follows:

1. A frontal passage is followed by a fresh air mass moving into the region encompassing the Hudson Valley and Catskill Plateau. On the first full day following the frontal passage, this air mass is characterized by a uniform vertical and horizontal distribution of temperature and moisture over the region, allowing for the development of a classic CBL, with little if any difference in the θ profile between the Valley and the Catskill Plateau.

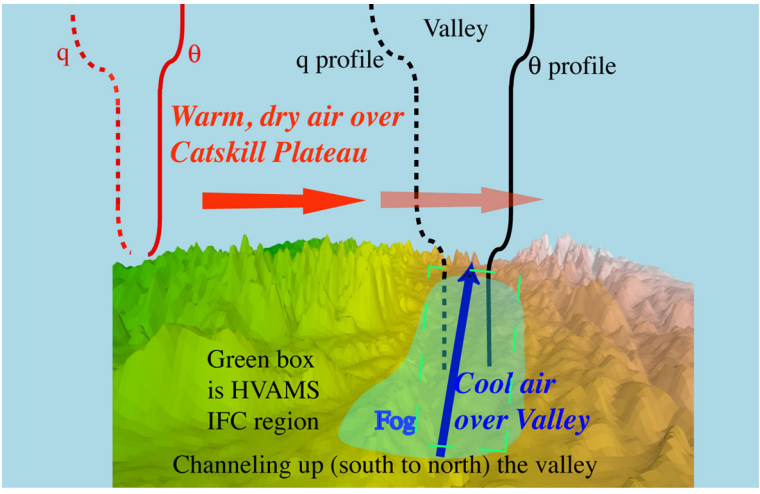

Fig. 12 Schematic of processes responsible for EML and valley-CBL coupling observed over the Hudson Valley. See text for explanation

2. On subsequent days, local processes (such as sensible and latent heat-flux convergence) produce a modification of the air mass (Freedman and Fitzjarrald 2001). These sequences typically last anywhere from 3 to 6 days.
3. Depending upon the time of year, differential heating of the Catskill Plateau (a result of the reduced evapotranspiration) produces higher temperatures over the higher terrain.
4. Within the Valley, cold-air pooling and fog formation delay the surface-layer inversion erosion and result in lower temperatures as compared with the Catskill Plateau; regional horizontal pressure differences and topography produce south-north (or north-south) channelled flow.
5. Above the Catskill Plateau and the valley CBL, westerly flow advects the regional EML over the valley.
6. These processes work together to establish the regional EML and valley-CBL coupling that is maintained by warm-air advection aloft and reduction of convective processes at the surface through the presence of fog or cold pools.

The synoptic weather systems that affected the region during the HVAMS intensive field campaign were not unusual. The regional EML and valley-CBL coupling was observed on 13 days of the 45-day campaign. This suggests that the regional EML and valley-CBL coupling is not a rare occurrence, at least during autumn. As channelling in the Hudson Valley is a key mechanism for pollutant transport near the surface (e.g., Fitzjarrald and Lala 1989), and the CBL depth is a determining variable in trace gas and particulate concentrations, the failure to capture this feature can lead to air-pollution concentration forecast errors in this populated region of New York State (Hogrefe et al. 2001; Rao et al. 2003; Yegorova et al. 2011). The regional EML and valley-CBL coupling also has implications for fog forecasting and wind shear, which in turn directly affect aviation and surface transportation interests within and adjacent to the Hudson Valley. It is likely that other valley/plateau topographic configurations experience similar regional EML and valley-CBL coupling, and therefore present model characterization and forecasting challenges.

Acknowledgements Primary support for this work is from the National Science Foundation through subcontract #1033027-1-28995 from the Research Foundation, State University of New York. We also appreciate the contributions made by John Sicker in providing overall technical support before, during, and after the intensive field campaign, Rodrigo da Silva, Ricardo Sakai and Kathleen Moore for invaluable field and technical support, then undergraduate students Jason Herb, Jessica Neiles, and Kimberly McMahon for providing much needed field and data support during project preparation, the intensive field campaign, and for the remainder of the HVAMS deployment, Jessie (Grimm) Beauharnois for critical administrative support, and the NWS Albany Forecast Office for providing additional rawinsonde launches and ASOS data during the intensive field campaign.

References

Adams AG (1996) The Hudson River guidebook. Fordham University Press, New York, 430 pp

Angevine WM, Baltink HK, Bosveld FC (2001) Observations of the morning transition of the convective boundary layer. Boundary-Layer Meteorol 101:209–227

Arritt RW, Wilczak JM, Young GS (1992) Observations and numerical modelling of an elevated mixed layer. Mon Weather Rev 120:2869–2880

Banacos PC, Ekster ML (2010) The association of the elevated mixed layer with significant severe weather events in the northeastern United States. Weather Forecast 25:1082–1102

Cai C, Hogrefe C, Katsafados P, Kallos G, Beauharnois M, Schwab JJ, Ren X, Brune WH, Zhou X, He Y, Demerjian KL (2008) Performance evaluation of an air quality forecast modeling system for a summer and winter season—photochemical oxidants and their precursors. Atmos Environ 42:8585–8599

Carlson TN, Benjamin SG, Forbes GS, Li Y-F (1983) Elevated mixed layers in the regional severe storm environment: conceptual model and case studies. Mon Weather Rev 111:1453–1474
Choi W, Faloona I, McKay M, Goldstein A, Baker A (2011) Estimating the atmospheric boundary layer height over sloped, forested terrain from surface spectral analysis during BEARPEX. Atmos Chem Phys 11(14):6837–6853
Czikowsky MJ (2003) Seasonal and successional effects on evapotranspiration and streamflow. M.S. thesis, Department of Earth and Atmospheric Sciences, The University at Albany, State University of New York, 105 pp [Available from M. Czikowsky in electronic form by request.]
Czikowsky MJ, Fitzjarrald DR (2004) Evidence of seasonal changes in evapotranspiration in eastern US hydrological records. J Hydrometeorol 5:974–988
Dai C, Wang Q, Kalogiros JA, Lenschow DH, Gao Z, Zhou M (2014) Determining boundary-layer height from aircraft measurements. Boundary-Layer Meteorol 152:277–302
De Wekker S (2002) Structure and morphology of the convective boundary layer in mountainous terrain. Ph.D. Dissertation, The University of British Columbia, BC, Canada, 191 pp
De Wekker S, Koßmann M (2015) Convective boundary layer heights over mountainous Terrain—a review of concepts. Front Earth Sci. doi:10.3389/feart.2015.00077
Emeis S, Schäfer K, Münkel C (2008) Surface-based remote sensing of the mixing-layer height—a review. Meteorol Z 17(5):621–630
Fitzjarrald DR, Lala GG (1989) Hudson valley fog environments. J Appl Meteorol 28:1303–1328
Fitzjarrald DR, Acevedo OC, Moore KE (2001) Climatic consequences of leaf presence in the eastern united states. J Clim 14:598–614
Foster DR (1992) Land-use history (1730–1990) and vegetation dynamics in central New England, USA. J Ecol 80:753–772
Freedman JM (2000) Vegetation–atmosphere interactions and boundary layer cumulus clouds. Ph.D. Dissertation. Department of Earth and Atmospheric Sciences, University at Albany, State University of New York, 143 pp
Freedman JM, Fitzjarrald DR (2001) Postfrontal airmass modification. J Hydrometeorol 2:419–437
Garratt JR (1992) The atmospheric boundary layer. Cambridge University Press, UK 316 pp
Groß G, Wippermann F (1987) Channelling and countercurrent in the upper Rhine Valley: numerical simulations. J Clim Appl Meteorol 26:1293–1304
Haeffelin M, Bergot T, Elias T, Tardif R, Carrer D, Chazette P, Colomb M, Drobinski P, Dupont E, Dupont J-C, Gomes L, Musson-Genon L, Pietras C, Plana-Fattori A, Protat A, Rangognio J, Raut J-C, Rémy S, Richard D, Sciare J, Zhang X (2010) PARISFOG, shedding new light on fog physical processes. Bull Am Meteorol Soc 91:767–782
Hogrefe C, Rao ST, Kasibhatla P, Kallos G, Tremback C, Hao W, Olerud D, Xiu A, McHenry J, Alapaty K (2001) evaluating the performance of regional-scale photochemical modeling systems: part I—meteorological model outputs. Atmos Environ 35:4159–4174
Hough FB (1855) Results of a series of meteorological observations made in obedience to instructions from the Regents of the University, at Sundry Academies in the State of New York
Ketterer C, Zieger P, Bukowiecki N, Coen CM, Maier O, Ruffieux D, Weingartner E (2014) Investigation of the planetary boundary layer in the Swiss Alps using remote sensing and in situ measurements. Boundary-Layer Meteorol 151(2):317–334
Laubach J, Fritsch H (2002) Convective boundary layer budgets derived from aircraft data. Agric For Meteorol 111:237–263
LeMone M, Grossman R, McMillen RT, Liou KM, Ou S, McKeen S, Angevine W, Ikeda K, Chen F (2002) CASES-97: late morning warming and moistening of the convective mixed layer over the Walnut River watershed. Boundary-Layer Meteorol 104:1–52
Lunny RM (ed) (1959) The voyage of the Half Moon from 4 April to 7 November 1609. Juet's journal. The New Jersey Historical Society, Newark, NJ, 37 pp
Mahrt L, Vickers D, Sun J (2001) Spatial variations of surface moisture flux from aircraft data. Adv Water Resour 2:1133–1141
Medeiros L, Fitzjarrald D (2014) Stable boundary layer in complex terrain. Part I: linking fluxes and intermittency to an average stability index. J Appl Meteorol Clim 53(9):2196–2215
Medeiros L, Fitzjarrald D (2015) Stable boundary layer in complex terrain. Part II: Geometrical and sheltering effects on mixing. J Appl Meteorol Clim 54(1):170–188
Meyer MB, Lala GG (1990) Climatological aspects of radiation fog occurrence at Albany, New York. J Clim 3:578–586
Moore KE, Fitzjarrald DR, Sakai RK, Goulden ML, Munger JW, Wofsy SC (1996) Seasonal variation in radiative and turbulent exchange at a deciduous forest in central Massachusetts. J Appl Meteorol 35:122–134

Rao ST, Zhang K, Ku M, Berman S, Mao H (2003) Summertime characteristics of the atmospheric boundary layer and relationships to ozone levels in the eastern United States. Pure Appl Geophys 160:21–55
Rendón A, Salazar J, Palacio C, Wirth V (2015) Temperature inversion breakup with impacts on air quality in urban valleys influenced by topographic shading. J Appl Meteorol Clim 54:302–321
Ruedemann R (1932) Development of drainage of Catskills. Am J Sci 23:337–349
Sakai RK, Fitzjarrald DR, Moore KE (1997) Detecting leaf area and surface resistance during transition seasons. Agric For Meteorol 84:273–284
Samson PJ, Neighmond G, Yencha AJJ (1975) The transport of suspended particulates as a function of wind direction and atmospheric conditions. J Air Pollut Control Assoc 25:1232–1237
Schmidli J (2013) Daytime heat transfer processes over mountainous terrain. J Atmos Sci 70:4041–4066
Serafin S, Zardi D (2011) Daytime development of the boundary layer over a plain and in a valley under fair weather conditions: a comparison by means of idealized numerical simulations. J Atmos Sci 68:2128–2141
Sofiev M, Prank M, Baklanov A (2011) Influence of regional scale emissions on megacity air quality. Technical report, FP7 EC MEGAPOLI project, 60 pp
Steinbacher M, Henne S, Dommen J, Wiesen P, Prevot AS (2004) Nocturnal trans-alpine transport of ozone and its effects on air quality on the Swiss Plateau. Atmos Environ 36:4539–4550
Thayer JS (1996) Catskill weather. Purple Mountain Press, Flesichmanns 167 pp
UCAR (2016) UCAR/NCAR—Earth Observing Laboratory, 1990-present. NCAR integrated surface flux system (ISFS). doi:10.5065/D6ZC80XJ
Wagner JS, Gohm A, Rotach MW (2014) The impact of horizontal model grid resolution on the boundary layer structure over an idealized valley. Mon Weather Rev 142:3446–3465
Wallace JM, Hobbs PV (2006) Atmospheric science: an introductory survey, 2nd edn. Academic Press, Cambridge 483 pp
Whiteman CD (1982) Breakup of temperature inversions in deep mountain valleys: part I. Observations. J Appl Meteorol 21:270–289
Yegorova EA, Allen DJ, Loughner CP, Pickering KE, Dickerson RR (2011) Characterization of an eastern U.S. severe air pollution episode using WRF/Chem. J Geophys Res 116:D17306